J Nanopart Res (2012) 14:929
DOI 10.1007/s11051-012-0929-y

RESEARCH PAPER

Aggregation of glutathione-functionalized Au nanoparticles induced by Ni^{2+} ions

R. Fu · J. Li · W. Yang

Received: 10 October 2011 / Accepted: 15 May 2012 / Published online: 8 June 2012

Abstract Aggregation of glutathione (GSH)-functionalized Au nanoparticles induced by Ni^{2+} ions were found to be related to pH of the solutions. At pH lower than 9.0, introduction of Ni^{2+} ions was less effective to induce aggregation of the Au nanoparticles. At pH around 9.8, the Au nanoparticles experienced extensive aggregation upon the addition of Ni^{2+} ions. When pH was higher than 10.5, Ni^{2+} ion-induced aggregation of the Au nanoparticles was suppressed gradually with increasing pH. It was identified that such pH-mediated aggregation behaviors are attributed to the different coordination fashions of GSH on the Au nanoparticle surface with Ni^{2+} ions. At pH lower than 9.0, addition of Ni^{2+} ions was less effective to induce aggregation of the Au nanoparticles when only the carboxyl group of the glutamyl residue was available for the metal ions. The Au nanoparticles underwent extensive aggregation at pH around 9.8 when both the carboxyl and deprotonated amine groups of the glutamyl residue in GSH could coordinate with the metal ions. At pH higher than 10.5, the coordination was gradually suppressed by the hydroxyl groups in solutions, addition of Ni^{2+} ions is less effective to cross-link the Au nanoparticles. Such a work is helpful for understanding the sensitivity and selectivity of GSH-functionalized Au nanoparticles to metal ions.

Keywords Au nanoparticles · Glutathione · Aggregation · Metal ions

Introduction

Au nanoparticles have been demonstrated to be a new kind of probes for colorimetric detection of metal ions (Cao et al. 2005; Elghanian et al. 1997; Hazarika et al. 2004; Ho and Leclerc 2004; Nam et al. 2003; Stojanavic and Landry 2002), which provides new chance to develop assay for quick detection of metal ions in the environmental and biomedical fields (Bal and Kasprzak 2002). After being functionalized by ligands with specificity to metal ions, the coordination between the ligands and metal ions induce the aggregation and thus color change of the Au nanoparticles, which provides the basis for qualitative and quantitative analyses of the metal ions (Darbha et al. 2008; Ghosh and Pal 2007; Hung et al. 2010; Huang et al. 2007; Huang and Chang 2007; Li et al. 2008, 2009, Slocik et al. 2008; Tan et al. 2009; Xue et al. 2008). During the past decade, a wide variety of ligands had been employed to functionalize Au nanoparticles and their performance as probes of metal ions had been evaluated. For examples, Au

Electronic supplementary material The online version of this article (doi:10.1007/s11051-012-0929-y) contains supplementary material, which is available to authorized users.

R. Fu · J. Li · W. Yang (✉)
State Key Laboratory of Supramolecular Structure and Materials, College of Chemistry, Jilin University, Changchun 130012, People's Republic of China
e-mail: wsyang@jlu.edu.cn

naoparticles functionalize by DNA-enzyme showed specific response to Pb^{2+} ions (Liu and Lu 2000, 2003, 2004; Swearingen et al. 2005), Au nanoparticles functionalized by oligo-DNA were sensitive to Hg^{2+} ions (Lee et al. 2007), histidine-functionalized Au nanoparticles had strong affinity to Fe^{3+} ions (Guan et al. 2008) etc. Glutathione (γ-Glu–Cys–Gly, GSH) is a tri-peptide with strong affinity to a wide variety of metal ions (Sudeep et al. 2005). However, GSH-functionalized nanoparticles were reported to show selectivity to definite metal ions. For examples, Fang et al. used GSH-functionalized Au nanoparticles to achieve selective detection of Pb^{2+} ions (Chai et al. 2010). Li et al. (2009) reported that GSH-functionalized Ag nanoparticles were responsive to Ni^{2+} ions. Kalluri et al. (2009) used GSH-functionalized Au nanoparticles to realize selective detection of As^{3+} ions in groundwater. Previous works have demonstrated that the coordination sites of GSH are tunable by pH (Bieri and Bürgi 2005). It is deduced that the selectivity may also be related to pH since the change in coordination sites of GSH will affect the affinity of the particles to metal ions. In this study, we investigated the aggregation behaviors of GSH-functionalized Au nanoparticles in presence of Ni^{2+} ions. It is revealed that such pH-mediated aggregation behaviors are attributed to the different coordination fashions of GSH on the Au nanoparticle surface with Ni^{2+} ions. At pH lower than 9.0, the Au nanoparticles showed poor sensitivity to Ni^{2+} due to its weak affinity to the carboxyl group of the glutamyl residue in GSH and better sensitivity to Cu^{2+} due to its strong affinity to the carboxyl group. At pH around 9.8, both the carboxyl and deprotonated amine groups of the glutamyl residue could coordinate with Ni^{2+}, which is effective to induce the extensive aggregation of Au nanoparticles. At pH higher than 10.5, the coordination is gradually suppressed by the hydroxyl groups in solutions, addition of Ni^{2+} ions is less effective to cross-link the Au nanoparticles.

Experimental

Materials

GSH (>98 %, $C_{10}H_{17}N_3O_6S$, FW 307.33), hydrogen tetrachloroaute(III) trihydrate (99.9+ %, $HAuCl_4 \cdot 3H_2O$, FW 393.8), sodium citrate tribasic dihydrate (≥99.0 %, $Na_3C_6H_5O_7 \cdot 2H_2O$, FW 294.1), nickel(II) sulfate heptahydrate (≥99 %, $NiSO_4 \cdot 7H_2O$, FW 280.86), and other metal ion containing reagents were purchased from Sigma-Aldrich and used as received. All solutions of metal ion containing reagents were prepared freshly before the experiments. Solution of reagent-grade NaOH (0.1 M) were used to adjust the pH value of the colloids. High-purity water (Pall Purelab Plus) with a resistivity of 18 MΩ cm was used in all the experiments.

Preparation of GSH-functionalized Au nanoparticles

Au colloids were prepared by sodium citrate reduction of chloroauric acid according to the modified Frens method (Ji et al. 2007). Typically, 100 mL solution of $HAuCl_4 \cdot 3H_2O$ (0.37 mM) was brought to boil under vigorous stirring in a round-bottom flask. A trisodium citrate (1.9 mM) solution was added, resulting in change in solution color from pale yellow to deep red. After the color change, the solution was heated for additional 15 min. After being isolated by centrifugation (8,000 rpm for 30 min), the Au colloid was re-dispersed in pure water and the original pH of the colloid was 6.5. Diameter of the as-prepared Au nanoparticles was determined to be 18 ± 2 nm by transmission electron microscopy (TEM) observations. To prepare glutathione-functionalized Au nanoparticles, 60 μL GSH was added into 1 mL of the as-prepared colloid whose pH value was previously adjusted to 9.0 using 0.1 M NaOH. After addition of glutathione and aging the Au colloid for 2.5 h, the mixture was washed twice with pure water to remove any uncoordinated GSH by centrifugation. The concentration of the GSH modified Au nanoparticles was 3.2 nM. Final pH value of the colloid was about 6.4 and adjusted to different pH values (7.0–12.0) with 0.1 M NaOH before the addition of 50 μM metal ions. The solution was incubated for 5 min after the addition of metal ions before the measurements.

Characterizations

FTIR spectra were recorded with a Perkin-Elmer Spectrum One FTIR spectrometer, performed by placing the CaF_2 windows with droplets of the solution in a cabin continuously purged with dry air.

UV-visible spectra were collected with a Varian Cary-100 scan UV–Vis spectrophotometer. Dynamic light scattering (DLS) measurements were performed using a particle size analyzer (BI-90 Plus, Brookhaven Instruments) with a scattering angle of 90°. TEM images were observed using a Hitachi H-8100 IV electron microscope at 200 kV using carbon-coated copper grids as substrates. Samples were prepared by dipping a drop of the colloidal solution (the aliquots taken during the course of a reaction) onto the grids. The photographs of the samples were caught by a Konica Minolta DiMAGE Z2 digital camera. All the experiments were carried out at room temperature (25 ± 2 °C).

Results and discussion

In the range of pH 6.4–12.0, the GSH modified Au nanoparticles were red in color, corresponding to a plasmon band at 520 nm. After the addition of 50 μM Ni^{2+}, the nanoparticles presented different absorption spectra under different pH (Fig. 1). For the nanoparticles with pH 6.4, almost no difference in absorption spectra was observable before and after the addition of Ni^{2+}. For the particles with pH 9.8, intensity of the plasmon band at 520 nm decreased evidently accompanied by the appearance of a new band at 610 nm after the addition of 50 μM Ni^{2+}, indicating the aggregation of the particles. At pH 12.0, the plasmon band underwent a slight red-shift and became a little broaden after the addition of 50 μM Ni^{2+}, suggesting the suppressed aggregation of the particles at this high pH. Such a conclusion can also be supported by the TEM observations (Fig. 2). At pH 6.4, the colloid kept the red color and the particles were well dispersed after the addition of Ni^{2+} ions. The average size of the particles was estimated to be about 28 nm as derived from DLS analyses (Fig. S1A in Supplementary material). At pH 9.8, color of the colloid was changed from red to purple and the particles aggregated extensively after the addition of Ni^{2+} ions. The average size of the aggregates was estimated to be about 168 nm as derived from the DLS analyses (Fig. S1B in Supplementary material). At pH 12.0, color of the colloid was changed from red to pink and the TEM image was dominated by small clusters of the particles. The average size of the particles was estimated to be about 38 nm as derived from the DLS analyses (Fig. S1C in Supplementary material).

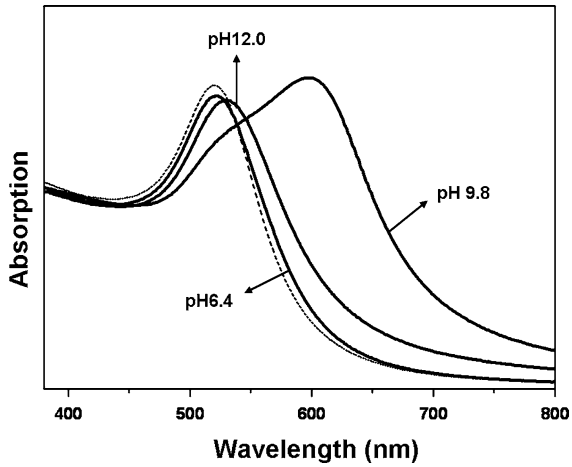

Fig. 1 UV–Visible spectra of the GSH-modified Au nanoparticles under pH 6.4, 9.8, and 12.0 in the presence of 50 μM Ni^{2+}. The *dashed line* represents the spectrum of the as-prepared GSH modified Au nanoparticles

Ratios of the absorbance intensity at 610 and 520 nm (E610/520), which represented the aggregated and free Au nanoparticles, respectively (Aslan et al. 2004) were calculated from the absorption spectra to further illustrate the effect of pH on aggregation of the Au nanoparticles induced by Ni^{2+} ions (Fig. 3). In the absence of Ni^{2+} ions, the ratios were lower than 0.2 in the range of pH 6.4–12.0, indicating the good stability of the particles in this range of pH (Fig. S2 in Supplementary material). In the presence of 50 μM Ni^{2+} ions, the ratios increased rapidly when pH of the colloid was higher than 9.0. It was likely that the effective aggregation of the particles was related to the deprotonation of the glutamyl amine group (pK = 8.7). At pH 12.0, the aggregation was suppressed greatly, which may be related to the increased concentration of hydroxyl groups (Jiang et al. 2009).

It is known that GSH is a multi-dentate ligand for metal ions. FTIR spectra of pure GSH and GSH loaded on the particle surface are given in Fig. 4. The strong band of –SH group at 2,525 cm^{-1} and the band of the –COOH group of the glycine residue at 1,713 cm^{-1} were not observable after loading of GSH onto the particle surface, indicating that GSH is anchored on the Au nanoparticles via its thiol group of the cysteine residue and the carboxylic acid group of the glycine residue (Bieri and Bürgi 2005). After being loaded onto the particle surface, the carboxyl and amine groups of the glutamyl residue are available sites for the metal ions. Protonation/deprotonization of the carboxyl and

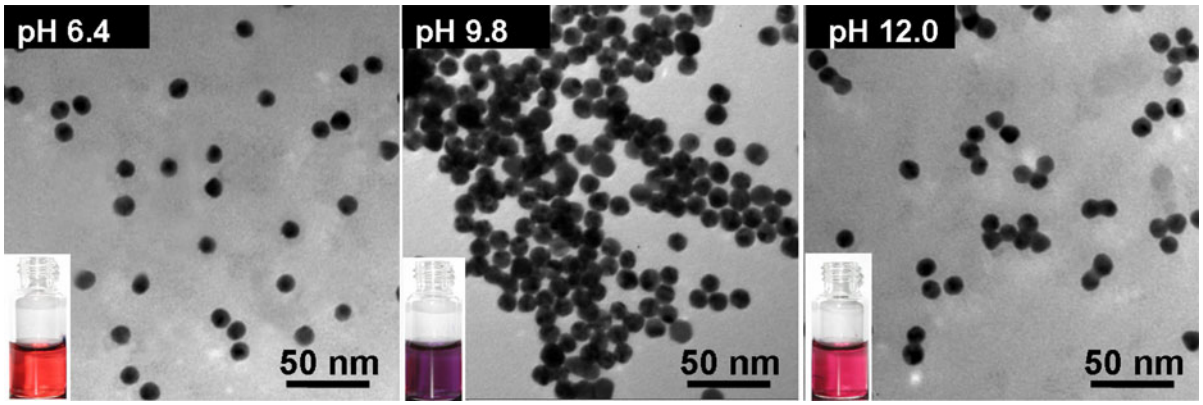

Fig. 2 TEM images of the GSH-modified nanoparticles with pH 6.4, 9.8, and 12.0 after the addition of 50 μM Ni^{2+}. *Inserts* give the corresponding photos of the Au colloids

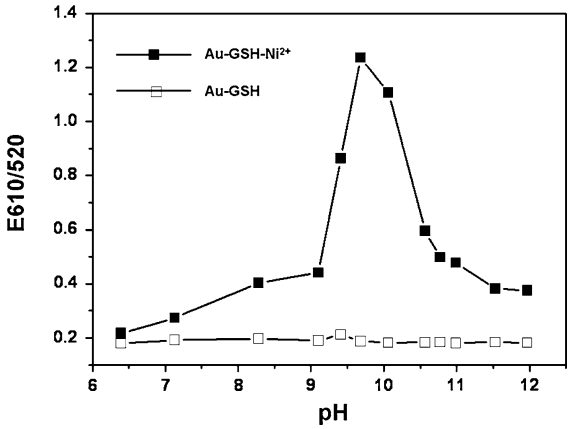

Fig. 3 Variation in the ratios of the absorbance intensity at 610 and 520 nm (E610/520) of the Au colloids with pH in the absence and presence of 50 μM Ni^{2+}

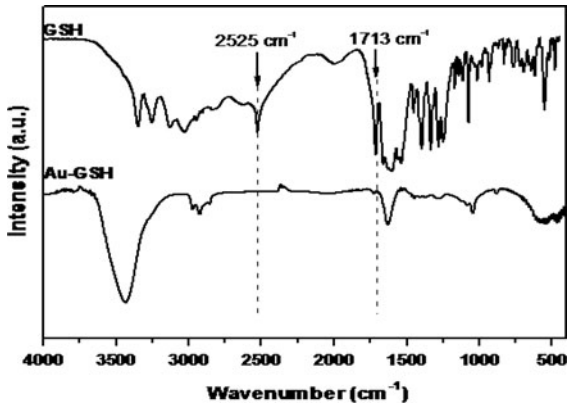

Fig. 4 FTIR spectra of pure GSH and GSH-modified Au nanoparticles

amine groups may result in different coordination fashions between Ni^{2+} and GSH (Zhang et al. 2010), thus promoting or suppressing aggregation of the particles. At pH 6.4, after the addition of Ni^{2+} ions, the symmetric and asymmetric C=O stretches of the glutamyl residue at 1,398 and 1,540 cm^{-1} shifted to 1,412 and 1,550 cm^{-1}, respectively (Fig. S3A in Supplementary material), indicating the coordination of Ni^{2+} with the carboxyl group (Bieri and Bürgi 2005; Krezel et al. 2003; Lim et al. 2008). The amine group (pK = 8.7) should not contribute to the coordination since it should exist in the protonated forms at this pH value (Dean 1999). At pH 9.8, GSH loaded on Au nanoparticle surface presented in-plane and out-of-plane deformations of N–H at 1,630 and 1,084 cm^{-1} from the deprotonated amine group of the glutamic residue. After the addition of Ni^{2+} ions, the vibrations shifted to 1,652 and 1,128 cm^{-1}, respectively (Fig. S3B in Supplementary material), suggesting that the amine group also participated in the coordination after its deprotonation (Krezel and Bal 2004; Krezel et al. 2003; Lim et al. 2008). It was noted that the symmetric and asymmetric C=O stretches of the glutamyl residue of GSH loaded on the particle surface also shifted from 1,410 and 1,530 cm^{-1} to 1,420 and 1,540 cm^{-1} after the addition of Ni^{2+} ions, indicating the carboxyl group of the glutamic residue still contributed to the coordination at this pH (Krezel and Bal 2004; Lim et al. 2008).

Variation in ratios of the absorbance intensity at 610 and 520 nm with concentration of Ni^{2+} ions was recorded to further understand the Ni^{2+} induced

aggregation processes of the Au nanoparticles (Fig. 5). At pH 6.4, there was almost no change of the ratio when the concentration of Ni^{2+} was lower than 80 μM, indicating that the added Ni^{2+} ions were primarily absorbed on surface of the Au nanoparticles. When the concentration of Ni^{2+} ions was higher than 80 μM, the ratio increased gradually with the increased concentration attributed to the cross-linking of the Au nanoparticles by Ni^{2+} ions. At pH 9.8, the cross-linking of the Au nanoparticles became dominant when the concentration of Ni^{2+} was higher than 10 μM. The ratio was proportional to the concentration of Ni^{2+} in the range of 10–80 μM, indicating that the GSH-modified Au nanoparticles were qualified for ratiometric detection of Ni^{2+} ions at this pH. When the concentration was higher than 80 μM, the ratio kept almost unchanged with the increased concentration of Ni^{2+}, possibly due to the competition effect of the hydroxyl groups. At pH 12.0, the ratio increased gradually with the increased concentration when the concentration of Ni^{2+} was lower than 50 μM. However, the slope of the curve at pH 12.0 was much smaller than that at pH 9.8, suggesting the suppressed cross-linking process of the Au nanoparticles by the increased concentration of hydroxyl groups at this high pH. When the concentration of Ni^{2+} was higher than 50 μM, there was no change of the ratio with the increased concentration of Ni^{2+} due to the competition effect of hydroxyl groups.

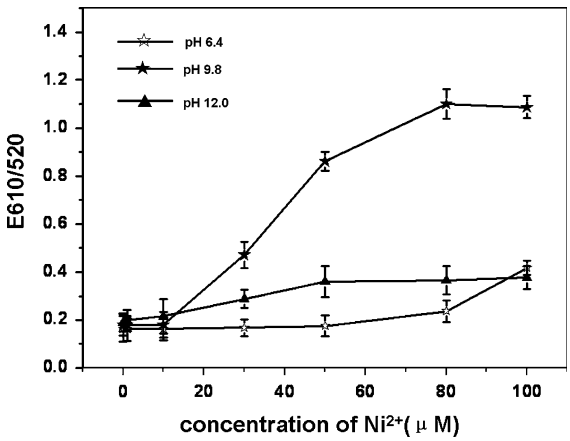

Fig. 5 Variation in ratios of the absorbance intensity at 610 and 520 nm (E610/520) of the Au colloids with concentrations of Ni^{2+} ions under pH of 6.4, 9.8, and 12.0.The *error bars* represent standard deviations based on five independent measurements

Based on above experimental results and discussion, the coordination fashions between GSH on the particle surface and Ni^{2+} under different pH were proposed as shown in Scheme 1. After being loaded onto the particle surface, the thiol and the carboxyl group of the glycyl residue are attached to the surface. At pH 6.4, only the carboxyl group of the glutamyl residue is available for Ni^{2+} ions, which is less effective to induce the cross-linking of the Au nanoparticles due to the relative weak affinity of the carboxyl group to Ni^{2+} (Log $K_{COO^-} = 1.81$). At pH 9.8, the coordination interactions between the Ni^{2+} and GSH ligand are effective to induce the aggregation of the Au nanoparticles when GSH acts as a bidentate ligand (Log $K_{COO^-} = 1.81$, Log $K_{NH_2} = 5.04$). At pH

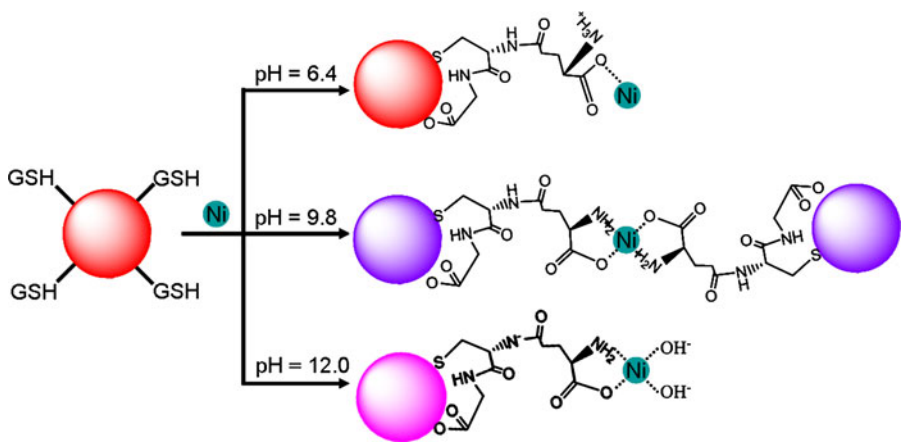

Scheme 1 Schematic representation of the coordination fashions between Ni^{2+} and GSH on the Au nanoparticle surface at pH 6.4, 9.8 and 12.0

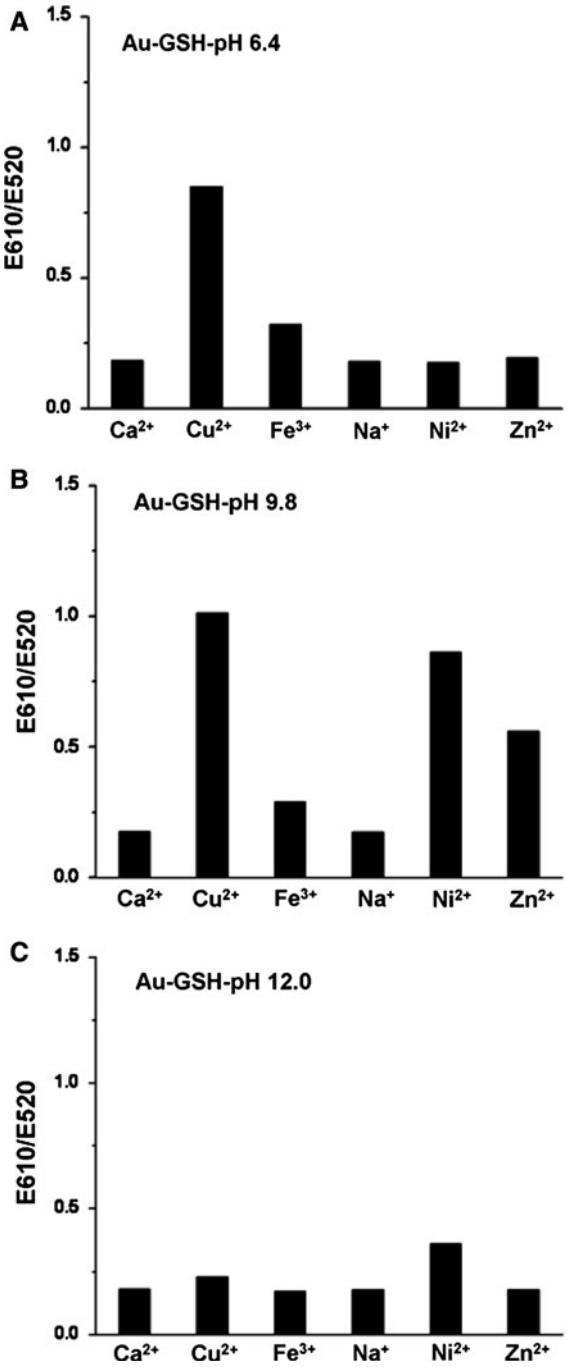

Fig. 6 Ratios of E620/E520 of the glutathione-functionalized Au nanoparticles at **A** pH 6.4 **B** pH 9.8 and **C** pH 12.0 in the presence of different metal ions (Ca^{2+}, Cu^{2+}, Fe^{3+}, Na^{+}, Ni^{2+}, Zn^{2+}). The concentration of each metal ion was 50 μM

12.0, the coordination between Ni^{2+} and GSH ligand is less effective to induce the cross-linking of the Au nanoparticles due to increased concentration of the hydroxyl groups, which may compete with the GSH and suppress the cross-linking.

Control experiments were carried out using other metal ions to further understand the aggregation behaviors of the Au nanoparticles. Figure 6 gives the ratio of E610/E520 recorded at different pH upon the addition of 50 μM metal ions. At pH 6.4, the Au nanoparticles were sensitive to the metal ions with strong affinity to carboxyl group, such as Cu^{2+} ions (Log $K_{COO^-} = 3.2$) and Fe^{3+} ions (Log $K_{COO^-} = 3.2$) (Dean 1999). The average sizes of the aggregates induced by Cu^{2+} and Fe^{3+} were estimated to be about 102 and 38 nm, respectively as derived from the DLS analyses (see Fig. S4A in Supplementary material). Other metal ions such as Ca^{2+} (Log $K_{COO^-} = 0.6$), Ni^{2+} (Log $K_{COO^-} = 1.81$) and Zn^{2+} (Log $K_{COO^-} = 1.50$) were less effective to induce the aggregation of the Au nanoparticles due to their weak affinity to the carboxyl groups. At pH 9.8, the metal ions with strong affinity to the deprotonated amine group, such as Ni^{2+} (Log $K_{NH_2} = 5.04$), Cu^{2+} (Log $K_{NH_2} = 7.98$), and Zn^{2+} (Log $K_{NH_2} = 4.81$), were more effective to induce the aggregation of the Au nanoparticles than those with weak affinity to the amine group for example Fe^{3+} (Log $K_{NH_2} = 2.20$) (Dean 1999). Average sizes of the aggregates induced by Ni^{2+} and Fe^{3+} were estimated to be about 180 and 45 nm, respectively (see Fig. S4B in Supplementary material). At pH 12.0, all the metal ions became less effective to induce the cross-linking of the Au nanoparticles due to the competition effect of the hydroxyl groups. Average sizes of the aggregates induced by Ni^{2+}, Fe^{3+}, and Cu^{2+} were smaller than 40 nm (see Fig. S4C in Supplementary material).

Conclusions

In this study, aggregation of the GSH-modified Au nanoparticles induced by Ni^{2+} ions was investigated. The difference in aggregation behaviors of the Au nanoparticles under different pH was related to the different coordination fashions between the GSH ligand and Ni^{2+}. At pH lower than 9.0, only the carboxyl group of the glutamyl residue in GSH could act as coordination site for metal ions, the Ni^{2+} ions are less effective to induce the aggregation of the Au nanoparticles due to their weak affinity to the carboxyl groups. At pH around 9.8, both the carboxyl and deprotonated amine groups of the glutamyl residue

could act as coordination sites, thus the Au nanoparticles undergo extensive aggregation upon the addition of Ni^{2+} ions due to their strong affinity to the amine groups. At pH higher than 10.5, the addition of Ni^{2+} ions is less effective to induce the aggregation of the Au nanoparticles due to the competition effect of the hydroxyl groups. Such a work should be helpful for understanding the sensitivity and selectivity of GSH-functionalized Au nanoparticles to various metal ions and designing the Au nanoparticles based probes for metal ions with better performance.

Acknowledgments This study was supported by the National Research Fund for Fundamental Key Project (No. 2009CB 939701, 2011CB935800) and the National Nature Science Foundation of China (21073078, 50825202).

References

Aslan K, Luhrs CC, Perez-Luna VH (2004) Controlled and reversible aggregation of biotinylated gold nanoparticles with streptavidin. J Phys Chem B 108:15631–15639. doi:10.1021/jp036089n

Bal W, Kasprzak KS (2002) Induction of oxidative DNA damage by carcinogenic metals. Toxicol Lett 127:55–62. doi:10.1016/S0378-4274(01)00483-0

Bieri M, Bürgi T (2005) L-Glutathione chemisorption on gold and acid/base induced structural changes: a PM-IRRAS and time-resolved in situ ATR-IR spectroscopic study. Langmuir 21:1354–1363. doi:10.1021/la047735s

Cao YC, Jin R, Thaxton CS, Mirkin CA (2005) A two-color-change, nanoparticle-based method for DNA detection. Talanta 67:449–455. doi:10.1016/j.talanta.2005.06.063

Chai F, Wang CG, Wang TT, Su ZM (2010) Colorimetric detection of Pb^{2+} using glutathione functionalized gold nanoparticles. Appl Mater Interface 2:1466–1470. doi:10.1021am100107k

Darbha GK, Singh AK, Rai US, Yu E, Yu HT, Ray PC (2008) Selective detection of mercury(II) ion using nonlinear optical properties of gold nanoparticles. J Am Chem Soc 130:8038–8043. doi:10.1021/ja801412b

Dean J A (1999) Lange's handbook of chemistry, 15th edn. McGraw-Hill Book Co., New York, p 884

Elghanian R, Storhoff JJ, Mucic RC, Letsinger RL, Mirkin CA (1997) Selective colorimetric detection of polynucleotides based on the distance-dependent optical properties of gold nanoparticles. Science 277:1078–1080. doi:10.1126/science.277.5329.1078

Ghosh SK, Pal T (2007) Interparticle coupling effect on the surface plasmon resonance of gold nanoparticles: from theory to applications. Chem Rev 107:4797–4862. doi:10.1021/cr0680282

Guan J, Jiang L, Li J, Yang WS (2008) pH-dependent aggregation of histidine-functionalized Au nanoparticles induced by Fe^{3+} ions. J Phys Chem C 112:3267–3271. doi:10.1021/jp7097763

Hazarika P, Ceyhan B, Niemeyer CM (2004) Reversible switching of DNA–gold nanoparticle aggregation. Angew Chem Int Ed 43:6469–6471. doi:10.1002/anie.200461887

Ho HA, Leclerc M (2004) Optical sensors based on hybrid aptamer/conjugated polymer complexes. J Am Chem Soc 126:1384–1387. doi:10.1021/ja037289f

Huang CC, Chang HT (2007) Parameters for selective colorimetric sensing of mercury(II) in aqueous solutions using mercaptopropionic acid-modified gold nanoparticles. Chem Commun 12:1215–1217. doi:10.1039/b615383f

Huang CC, Yang Z, Lee KH, Chang HT (2007) Synthesis of highly fluorescent gold nanoparticles for sensing mercury(II). Angew Chem Int Ed 46:6824–6828. doi:10.1002/anie.200700803

Hung YL, Hsiung TM, Chen YY, Huang CC (2010) A label-free colorimetric detection of lead ions by controlling the ligand shells of gold nanoparticles. Talanta 82:516–522. doi:10.1016/j.talanta.2010.05.004

Ji XH, Song X, Li J, Bai Y, Yang WS, Peng XG (2007) Size control of gold nanocrystals in citrate reduction: the third role of citrate. J Am Chem Soc 129:13939–13948. doi:10.1021/ja074447k

Jiang L, Guan J, Zhao L, Li J, Yang WS (2009) pH-dependent aggregation of citrate-capped au nanoparticles induced by Cu^{2+} ions: the competition effect of hydroxyl groups with the carboxyl groups. Colloids Surf A 346:216–220. doi:10.1016/j.colsurfa.2009.06.023

Kalluri JR, Arbneshi T, Khan SA, Neely A, Candice P, Varisli B, Washington M, McAfee S, Robinson B, Banerjee S, Singh AK, Senapati D, Ray PC (2009) Use of gold nanoparticles in a simple colorimetric and ultrasensitive dynamic light scattering assay: selective detection of arsenic in groundwater. Angew Chem Int Ed 48:9668–9671. doi:10.1002/anie.200903958

Krezel A, Bal W (2004) Studies of zinc(II) and nickel(II) complexes of GSH, GSSG and their analogs shed more light on their biological relevance. Bioinorg Chem Appl 2:293–305. doi:10.1155/s1565363304000172

Krezel A, Szczepanik W, Sokolowska M, Jezowska-Bojczuk M, Bal W (2003) Correlations between complexation modes and redox activities of Ni(II)–GSH complexes. Chem Res Toxicol 16:855–864. doi:10.1021/tx034012k

Lee JS, Han MS, Mirkin CA (2007) Colorimetric detection of mercuric ion (Hg^{2+}) in aqueous media using DNA-functionalized gold nanoparticles. Angew Chem Int Ed 46:4093–4096. doi:10.1002/anie.200700269

Li D, Wieckowska A, Willner I (2008) Optical analysis of Hg^{2+} ions by oligonucleotide-Au nanoparticles hybrids and DNA-based machines. Angew Chem Int Ed 47:3927–3931. doi:10.1002/anie.200705991

Li HB, Cui ZM, Han CP (2009) Glutathione-stabilized silver nanoparticles as colorimetric sensor for Ni^{2+} ion. Sens Actuators B 143:87–92. doi:10.1016/j.snb.2009.09.013

Lim IS, Mott D, Ip W, Njoki PN, Pan Y, Qin S (2008) Interparticle interactions in glutathione mediated assembly of gold nanoparticles. Langmuir 24:8857–8863. doi:10.1021la800970p

Liu J, Lu Y (2000) A highly sensitive and selective catalytic DNA biosensor for lead ions. J Am Chem Soc 122:10466–10467. doi:10.1021ja0021316

Liu J, Lu Y (2003) A colorimetric lead biosensor using DNAzyme-directed assembly of gold nanoparticles. J Am Chem Soc 125(22): 6642–6643. doi:10.1021/ja034775u

Liu J, Lu Y (2004) Accelerated color change of gold nanoparticles assembled by DNAzymes for simple and fast colorimetric Pb^{2+} detection. J Am Chem Soc 126:12298–12305. doi:10.1021ja046628h

Liu J, Cao Z, Lu Y (2009) Functional nucleic acid sensors. Chem Rev 109:1948–1998. doi:10.1021cr030183i

Nam JM, Thaxton CS, Mirkin CA (2003) Nanoparticle-based biobarcodes for the ultrasensitive detection of proteins. Science 301:1884–1886. doi:10.1126science.1088755

Slocik JM, Zabinski JS, Phillips DM, Naik RR (2008) Colorimetric response of peptide-functionalized gold nanoparticles to metal ions. Small 4:548–551. doi:10.1002smll.200700920

Stojanavic MN, Landry DW (2002) Aptamer-based colorimetric probe for cocaine. J Am Chem Soc 124:9678–9679. doi:10.1021/ja0259483

Sudeep PK, Joseph STS, Thomas KG (2005) Selective detection of cysteine and glutathione using gold nanorods. J Am Chem Soc 127:6516–6517. doi:10.1021ja051145e

Swearingen CB, Wernette DP, Cropek DM, Lu Y, Sweelder JV, Bohn PW (2005) Immobilization of a catalytic DNA molecular beacon on Au for Pb(II) detection. Anal Chem 77:442–448. doi:10.1021ac0401016

Tan ZQ, Liu JF, Liu R, Yin YG, Jiang GB (2009) Visual and colorimetric detection of Hg(2+) by Cloud point extraction with functionalized gold nanoparticles as a probe. Chem Commun 45:7030–7032. doi:10.1039b915237g

Xue XJ, Wang F, Liu XG (2008) One-step, room temperature, colorimetric detection of mercury (Hg^{2+}) using DNA/nanoparticle conjugates. J Am Chem Soc 130:3244–3245. doi:10.1021ja076716c

Zhang J, Li J, Zhang JX, Xie RG, Yang WS (2010) Aqueous synthesis of ZnSe nanocrystals by using glutathione As ligand: the pH-mediated coordination of Zn^{2+} with glutathione. J Phys Chem C 114:11087–11091. doi:10.1021jp102540w